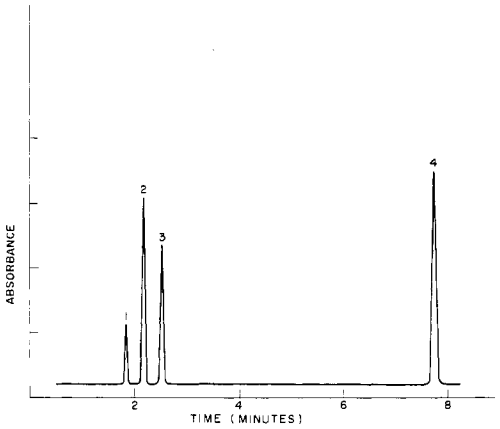

Figure 1. Separation of diazonium salts with acetonitrile–buffer eluent on μBondapak C-18

Peaks (1, 2), *p-N,N*-diethylaminobenzenediazonium chloride; (3), 3-methyl-4-pyrrolidinylbenzenediazonium chloride; (4), 2,5-di-*n*-butoxy-4-morpholinobenzenediazonium chloride

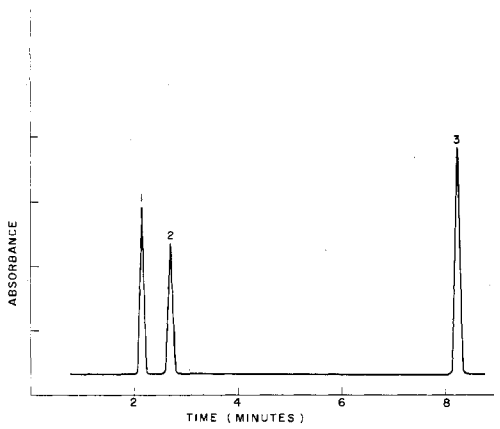

Figure 2. Separation of diazonium salts in acetonitrile–buffer with heptanesulfonate added

Peak (1), *p-N-N*-diethylaminobenzenediazonium chloride; (2), 3-methyl-4-pyrrolidinylbenzenediazonium chloride, (3) 2,5-di-*n*-butoxy-4-morpholinobenzenediazonium chloride

Muskegon, Mich. The diazonium salts were commercial sensitizers supplied by Philip Hunt and ABM Chemicals Ltd. and recrystallized several times.

Apparatus. Chromatography was performed on a Waters C-900 3000 PSI pumping system with a Valco CV-6-HPAX sampling valve and a Waters Model 440 ultraviolet detector. The column was a Waters 30 cm × 5 mm μBondapak C-18 column. Chromatograms were integrated with a Spectra Physics Minigrator.

Procedure. One-percent solutions of the diazonium salts were made up in water and stabilized with 1% citric acid. They were diluted 5:50 in acetonitrile along with a 10% toluene internal standard diluted 2:50 and injected in the 10-μl sample loop.

The buffer consisted of 2.5% potassium phosphate monobasic with phosphoric acid added to obtain a PH of 3.

RESULTS AND DISCUSSION

2,5-Di-*n*-butoxy-4-morpholinobenzenediazonium chloride, ½ (zinc chloride) and 3-methyl-4-pyrrolidinylbenzenediazonium chloride, ½ (zinc chloride) yielded sharp quantitative peaks on the octadecyl column using 45 acetonitrile–55 aqueous PH3 buffer as eluent at a flow rate of 1.3 ml/min. However, *p-N,N*-diethylaminobenzenediazonium chloride, ½ (zinc chloride) yielded two peaks, as in Figure 1. Addition of 0.005 M heptanesulfonic acid to the buffer–acetonitrile eluent resulted in one sharp peak, as in Figure 2. The precision was 0.2% standard deviation with good least squares linearity (0.9988 coefficient of determination) over a range of 0.07 to 0.14% diazonium salt after dilution. The quantitative data were obtained by area ratio of the peak to the toluene internal standard.

CONCLUSIONS

The diazonium ion probably exists as an ion pair in this system and the double peak of the *p-N,N*-diethylaminobenzenediazonium salt may be the result of ion pairs with two anions. Formation of the heptanesulfonate ion pair resulted in one peak. The retention time of the last salt, which was well retained, was increased significantly when heptanesulfonate was added as expected, but the first two salts which elute rapidly were not significantly more retained as heptanesulfonates.

This system is also useful for separation of diazonium salts and couplers in reprographic formulations. The degree of quantitation is excellent for quality control application.

LITERATURE CITED

(1) R. F. Borch, *Anal. Chem.*, **47**, 2437 (1975).
(2) M. Dong, D. Locke, and E. Ferrand, *Anal. Chem.*, **48**, 368 (1976).
(3) D. P. Wittmer, N. O. Nuessle, and W. G. Haney, *Anal. Chem.*, **47**, 1422 (1975).

RECEIVED for review May 19, 1976. Accepted July 6, 1976.

Analysis of Solid Materials by Laser Probe Mass Spectrometry

R. A. Bingham

AEI Scientific Apparatus Ltd., Barton Dock Road, Urmston, Manchester, England

P. L. Salter*

Department of Applied Physics, University of Hull, Hull, Yorkshire, England

Three types of laser have been examined as sources of ion production for trace element analysis of solid materials by mass spectrometry. Comparison is made between the lasers and with the conventional rf spark source. Their analytical qualities and potential are discussed for the examination of both conducting and nonconducting materials.

The conventional means of ionizing solid materials for the analysis of trace elements in mass spectrometry is by the radio-frequency spark (*1*). The laser has an appeal as a competitor because of its inert nature and because it provides the possibility of examining small regions of single specimens without the need for special preparation. In the case of the

Table I. Pulsed Laser Parameters

	CO_2 gas	Ruby	NdYAG
Pulse length, ns	>100	20	15
Energy, mJ	300	10	10
Q-switched	...	Dye—Vanadyl phthalocyanine	Pockells cell
Wavelength, μm	10.6	0.6943	1.06
Pulse repetition rate	Up to 1 Hz	10 s per pulse (max)	Up to 50 Hz
Mode	Multimode	Single TEM_{00}	Single TEM_{00}
Pulse reproducibility	...	±15%	±5%

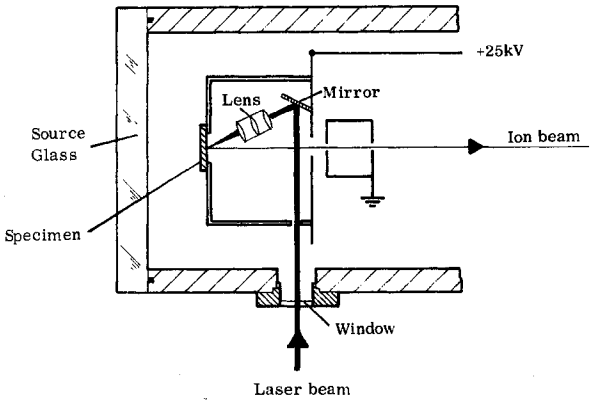

Figure 1. Mass spectrometer source arrangement

spark source, a pair of electrodes must be prepared which are electrically conducting. This can present problems for both solid and powder samples. For solids, the surfaces can be contaminated from handling or from chemical reagents used for etching and cleaning the surfaces. In the case of nonconducting powders, these have to be mixed with a high purity conducting powder, usually graphite, silver, or aluminum. This has two detrimental effects. First, the material for examination is atomically diluted by a function of the weight mix and the atomic weights of the two materials involved, thus reducing analysis sensitivity. Second, any trace elements in the conducting powder will limit the analysis sensitivity of these elements in the sample. The use of the laser as a means of ionizing the material overcomes these problems as the specimen may be examined directly and in many cases without any preparation. The electrical conductivity of the sample has little influence on ion production.

INSTRUMENTAL

In a previous paper (2), we have demonstrated the quantitative analytical capability of the ruby laser for solid materials and shown that it provides not only a microanalytical surface technique because of its small beam diameter capability but also offers the possibilities of both bulk and surface analysis with a focused or defocused beam. In this paper, we report on work carried out using three types of high power pulsed laser source; CO_2, ruby, and NdYAG; and we compare these with the conventional spark source. We have not used any secondary ionizing process in our work but have extracted ions directly from the laser-produced plasma into an AEI MS7 type double-focusing mass spectrometer. This instrument is of the Mattauch-Herzog design normally used with the spark source which is capable of coping with the large ion energy spread produced by the spark and it was expected to be more than adequate for the anticipated energy spread from ions of a laser plasma.

We have concluded that the ideal laser for materials analysis is a pulsed laser operated in the Q-switched mode. With a Q-switched laser, a high intensity short duration pulse interacts with the sample. Material is removed early in the pulse and the energy of the pulse is used in the efficient ionization of the evaporated material (3). A highly ionized plasma is produced which expands away from the sample surface. The use of a high intensity short duration pulse is advantageous for the following reasons. If the pulse length is long, the plasma temperature increases and so do the ionization states resulting in large numbers of multiply charged ions. Also, since the plasma lifetime is long, radiation from the plasma can cause local evaporation around the crater which can boil out volatile elements. Furthermore, a low laser power density ($<10^8$W cm^{-2}) can be shown to discriminate against higher boiling point elements to the advantage of the volatile elements.

Our work has been carried out mainly in the power density range 10^9–10^{11} W cm^{-2} and, at these high fluxes, the laser is found to be nonselective for a wide range of elements.

EXPERIMENTAL

Figure 1 is a schematic layout of the mass spectrometer source housing and shows how it has been modified for the ruby and NdYAG laser systems. The specimen is mounted with its plane normal to the mass spectrometer and the laser beam is passed through a window in the wall of the chamber, reflected from a mirror through a lens system to strike the specimen surface at an angle of approximately 45°. Both the lens and the specimen positions can be adjusted from outside the vacuum chamber to give control of the position of the specimen and focus of the beam. Generally, the focal point of the laser beam is arranged to coincide with the specimen surface in line with the optical axis of the mass spectrometer but this is not critical. As will be explained in more detail later, the experimental arrangement was slightly different when the CO_2 laser was used as at the wavelength of its radiation (λ = 10.6 μm) germanium optical components were necessary. A viewing system incorporating a microscope is also fitted to the source chamber and provides a large field of view of the region to be examined. The area for analysis is selected using a He–Ne C.W. laser which is aligned along the same optical path as the pulsed laser. This method of alignment is found to be quite accurate for selecting small regions for analysis. Crater diameters down to 20 μm have been obtained with the ruby and NdYAG laser systems.

All results reported in this paper have been recorded on Ilford Q2 photoplates. These are ideal detectors for experimental work as they can detect all isotopes over the mass range 6–240 simultaneously with the MS7 and enable the effects on all types of ion species to be observed. Photoplates do not have the sensitivity of electrical detection techniques but are much more useful for overall assessment purposes.

All three lasers used in the experiments produced large pulses of ions (of the order of several amperes) and it was necessary to support the accelerating voltage (25 kV) with capacitors. Shielding was necessary to screen the plasma from earthed parts of the source chamber to avoid accelerating voltage collapse which would reduce ion transmission through the mass spectrometer. Space charge problems were also experienced in the ion beam within the mass spectrometer and this was overcome by closing the object slit of the mass spectrometer (S3) down to 10-μm width. The resolving power thus obtained with all three lasers was similar to that of the spark source.

Details of the parameters of the three lasers are given in Table I.

CO_2 Laser. The laser used was a CO_2 solid cathode Transversely Excited Atmospheric gas laser. This type of laser has been described by Pearson and Lamberton (4). The main discharge occurred across two parallel electrodes with edges shaped to a Rogowski profile. Initial ionization is produced by field emission from a fine trigger wire which runs parallel to the two electrodes. Field emission induces a sheet

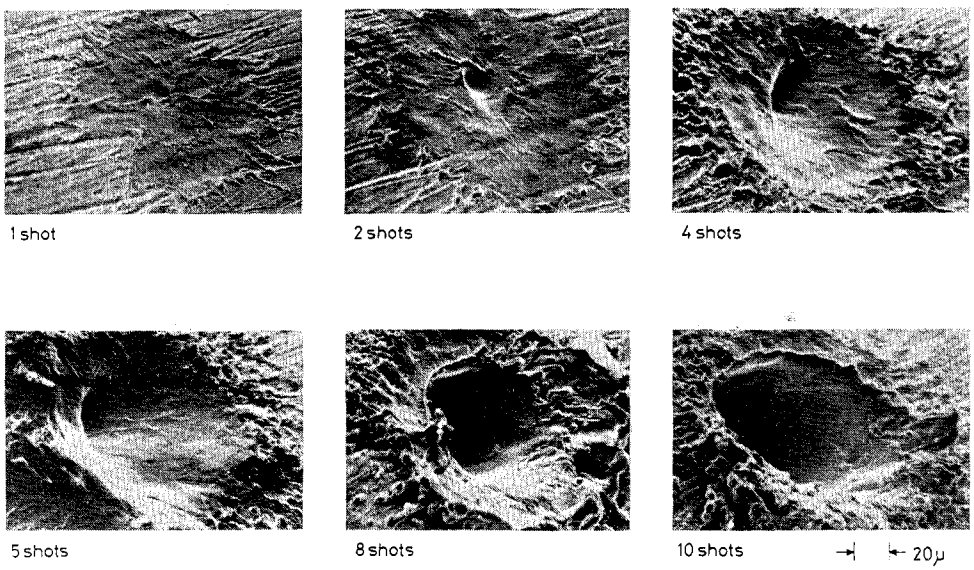

Figure 2. Ruby laser craters

Table II. Ruby Laser Power Density

Focused spot diameter μm	Power, density, W cm^{-2}
500	10^8
160	10^9
50	10^{10}
20	10^{11}

discharge across the whole length of the electrodes. The laser was a sealed unit having a discharge length of 28 cm. This meant that no control over the output mode structure was possible. The multimode output of the laser had a peak pulse of about 300 mJ. The pulse shape as observed using a photon drag detector has a fairly narrow initial peak (half width 100 ns) and a long tail of between 1 and 4 μs.

A considerable amount of energy occurred in the tail of the pulse. The laser was not Q-switched but the maximum power density in the initial peak of the pulse was of the order of 10^9 W cm^{-2}. As was noted earlier, it was necessary to use germanium optical components to transmit the radiation (λ = 10.6 μm) into the mass spectrometer source. The radiation was focused using a 1.5-in. (3.8-cm) focal length germanium lens and the crater sizes obtained were approximately 300 μm in diameter (on mild steel). Typical crater depths were 10 μm. Because of the multimode output of the laser, the intensity distribution across the focused beam was not uniform and "hot spots" or lobes occurred. The effects of these could be observed in the craters produced.

Visual element sensitivity on the photoplate was 2000 ppm atomic per laser shot from materials such as steel and was obtained from a crater 300 μ in diameter and 10 μm deep. By repeating a series of shots, all superimposed on the same spectrum, a higher sensitivity is obtained. Thus, 1000 shots produced sensitivity of 2 ppm and with a pulse repetition rate of 1 Hz the 1000 pulses took 16 min to record.

Using the CO_2 laser under these conditions, volatile elements were found to be preferentially emitted and some substances, such as copper, were low in ion production. This could be expected as copper is known to be highly reflective to the longer wavelengths.

Semiquantitative analysis could be carried out but the relative sensitivity factors of the elements covered a wide range. These aspects will be discussed later. The large amounts of material removed showed an ionization efficiency of about 1% despite there being several levels of multiply charged ion species present in the spectra.

Ruby Laser. Some of the work carried out with the ruby laser has been reported in a previous paper (*2*). In this paper we will present further results and highlight its differences with the other laser sources. The NdYAG and ruby laser are found to be very similar in most respects and their parameters are given in Table I. The ruby laser had a low pulse repetition rate of 1 pulse every 10 s and gave a photoplate sensitivity of 1000 ppm per shot. So to fire 300 shots (the largest number recorded) in order to reach a visual photoplate sensitivity of 3 ppm required a time of 50 min.

The reproducibility of the pulse output was estimated to be ±15% using a photodiode measuring system. The amount of material evaporated, for the same element sensitivity was considerably lower with the ruby laser than with the CO_2 laser. This is to be expected for a Q-switched laser (*3*). A single laser pulse on mild steel evaporated about 10^{-8} g of steel compared with 6×10^{-7} g with the CO_2 laser.

NdYAG Laser. This was a commercial laser system which had a pulse repetition rate which could be controlled over the range from single pulses to 50 Hz. This feature provided several advantages over the other lasers. The major advantage was the greater speed of analysis, but it also offers the possibility of using electrical detection methods for either spectrum scanning or peak switching. With the higher pulse repetition rate, it was possible to use the ion monitor signal on the MS7 as a measure of transmission, and it was reasonably steady at repetition rates above 20 Hz. This stable signal made it much easier to tune the mass spectrometer for optimum transmission.

A single shot from the NdYAG laser gave a visual sensitivity on the photoplate of 1000 ppm and the spectra showed good quantitative features.

The power density at the specimen surface is a function of the focus conditions for a fixed pulse energy, and Table II gives an indication of the levels used in these experiments. Most work has been carried out in the power density range 10^9–10^{11} W cm^{-2}. Latest work has shown that pulses of about 10^{14} ions are produced in each laser pulse and the ionization efficiency measured approaches 100%.

Crater dimensions can be varied over the range 20–300 μm diameter with depths of 5 μm at 20 μm diameter in steel down to 0.5 μm at 300 μm. Figure 2 shows a set of six electron microscope photographs of the ruby laser craters produced by increasing numbers of laser shots on steel.

The laser beam is incident at an angle of 45° to the steel surface and was "in focus" on the surface.

The output of both the ruby and NdYAG lasers is single mode. The beam intensity profile is Gaussian and, therefore, the highest power density occurs in the center of the laser produced crater. The power density falls off at the edges of the beam and consequently there is a region around the rim of the crater where only melting occurs. Material which is explosively removed from the center of the crater also re-solidifies around the edge of the crater. This is seen in the electron microscope photographs shown in Figure 2. The outer region produced by melting can be reduced by using an aperture in the laser beam. This is illustrated in Figure 3 which shows a single shot ruby crater in steel. The outer molten region has been almost completely eliminated. No detectable reduction in ion pulse intensity was noticed using this technique and it tended to confirm our observations that few ions are produced from the outer regions of the crater.

It is not important for specimen surfaces to be flat. We have examined such things as irregular fractured rock surfaces selecting individual mineral grains with little loss in ion signal; but if the angle between the specimen and the optical axis of the mass spectrometer is large, then ion extraction does suffer. This aspect and also the small probe size enables very small specimens to be examined either embedded in some other bulk material or mounted on the end of a pin or rod.

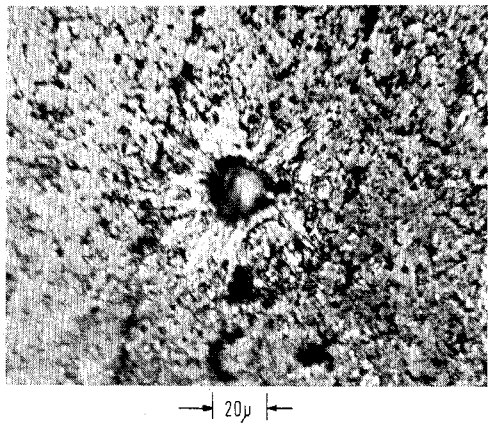

Figure 3. Single shot ruby laser crater in steel

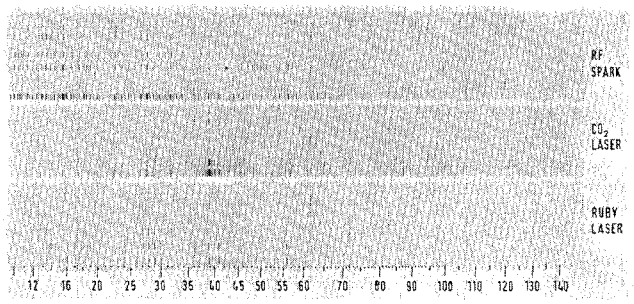

Figure 4. Rock specimen of slate

With the ruby and NdYAG lasers, ion extraction is just as efficient with electrically nonconducting as with conducting materials. Substances such as glass produce ion pulses of the same magnitude as metallic samples, and no problems are encountered due to surface charging as found in other probe techniques. We have also examined solid organic materials directly although the lasers rapidly dig deep holes.

We have obtained good spectra from rubber and have examined plastics, wood, walnuts, and other similar substances. We have only detected carbon and oxygen in these fairly pure organic materials. This feature could open up new fields of application in the mass spectrometry of organic solids.

Sensitivity of element detection is achieved by superimposing several laser pulses on one spectrum. A single ruby or NdYAG laser shot has a sensitivity of 1000 ppm and in the case of steel this removes 10^{-8} g of material. We have found this relationship to be linear up to the maximum number of shots recorded of 300 pulses for the ruby laser. Using the NdYAG system with a well focused beam over a large number of shots, the ion signal falls as the crater deepens because of the angle between the laser beam and specimen surface with respect to the optical axis of the mass spectrometer. As the crater deepens, the ions expand back along the laser beam. With a defocused beam, this effect is reduced; and extrapolating from our figures for a single shot of 1 pulse removing 10^{-8} g for 1000-ppm detection level, one may expect that at 50 Hz then 10^5 pulses would remove 1 mg to give a sensitivity of 0.01 ppm in 33 min. These figures are similar to that currently achieved by the spark source for the same exercise. In practice, it is unlikely to compare as favorably because of the cratering effects previously discussed, but could certainly compete on shorter less sensitive analyses.

Although electrical detection techniques have not yet been employed for analysis of the laser ion beams, a higher instantaneous sensitivity for individual elements could be obtained giving up to a factor 10^3 gain and providing a detection limit of about 1 ppm for a single shot. With a repetition rate of 30–50 Hz, the spectrum could be scanned over a large mass range or selected elements peak switched in a similar manner to that currently used with the spark source and with detection limits of the same order (0.1 ppm scanning; 0.01 ppm peak switching).

RESULTS AND DISCUSSION

The spectra obtained with the laser sources are not as complex as the spark source, and the resolving power is similar

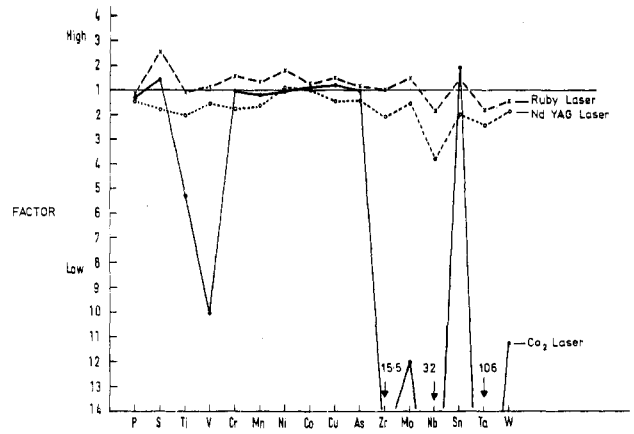

Figure 5. Laser sensitivity of elements relative to matrix-steel

giving around 3000 at mass 60 (50% peak height definition) under present conditions. Multiply charged ions are present in the laser spectra but are at lower levels than the spark.

Figure 4 shows spectra over the mass range 10–150 obtained from a specimen of slate using spark, CO_2, and ruby laser ion sources. Each set of spectra are from a separate photoplate, each recorded in steps 1–3–10, etc. The spark spectra have been recorded as charge over the range 0.01–3 nC, the CO_2 laser spectra over the range 1–1000 shots, and the ruby laser 1–300 shots.

The dispersions of the three sets of spectra are not quite the same and so have been lined up at *m/e* 40. It can be seen that the spark spectra are rich in lines at the lower mass range because of multiply charged ions compared with those of the lasers. For example, the doubly charged ion species ^{39}K and ^{41}K found at *m/e* 19.5 and *m/e* 20.5 are very much less dense in the laser spectra than the spark. Molecular species have rarely been found in the laser spectra, even in such complex substances as this rock indicating the high energy processes taking place in the plasma.

Slate is a good example of a nonconducting complex mineral mixture and demonstrates well the differences between these sources. The major elements are oxygen, silicon, aluminum, and potassium with smaller amounts of magnesium, sulfur and iron. An interesting feature of these spectra is that the small probe size of the ruby laser has picked out a small crystal of iron pyrite (FeS). The second spectrum (3 shots) of the ruby series shows strong ^{56}Fe and ^{32}S compared with their absence in the single- and ten-shot spectra. The crystal must have weighed less than 3×10^{-8} g and been of the order of a 20-μm cube in size. The CO_2 laser and spark sources cover a much larger surface area and are unable to discriminate to such small dimensions.

The CO_2 laser spectra show the typical thermal effects on element selectivity of the more volatile elements as can be seen for potassium (*m/e* 39/41), rubidium (*m/e* 85/87) and cesium (*m/e* 133). They are grossly enhanced in comparison with the spark and ruby spectra and can be attributed to the lower peak power density and long tail of the laser pulse.

The problem of element sensitivity (normally termed the relative sensitivity factor) is a measure of the sensitivity of an element with respect to the matrix element(s). For example, a volatile element such as sodium in aluminum could show a high value of sodium with respect to the aluminum, whereas an element like tungsten could appear unexpectedly low. The relative sensitivity factors for a range of elements in a steel standard have been measured for the CO_2, ruby, and NdYAG lasers and are shown in Figure 5. To retain linearity of comparison the measurements below unity are reciprocals of the value Calculated Value/Nominal Value used to obtain the factors. It can be seen that the relative sensitivity factors for

Table III. Visual Analysis of NBS Steel Standard 467 with the MS7/NdYAG Laser (ppm weight)

Element	Concentrations	
	Given	Calculated
Pb	6	11
W	2000	2300
Ta	2300	970
Sn	1000	1260
Mo	210	350
Nb	2900	1660
Zr	940	490
Ag	40	116
As	1400	1340
Ge	30	77
Cu	670	1030
Ni	880	1580
Co	740	1050
Mn	2800	2950
Cr	360	460
V	410	460
Ti	2600	5150
S	100	57
B	2	0.7

Table IV. Visual Analysis of Johnson-Matthey Copper Standard CAO with the MS7/NdYAG Laser (ppm weight)

Element	Concentration	
	Given	Calculated
Bi	500	326
Pb	400	323
Sb	500	381
Sn	480	276
Ag	470	338
Ga	350	387
Cr	220	120

the ruby and NdYAG lasers are close to unity. They are very similar to each other and to those obtained for the spark source. However the CO_2 laser shows poor sensitivity for the high boiling point elements, particularly niobium and tantalum where the latter is over a factor of 100 down.

High relative sensitivity factors are not serious if they are constant, and can be quantitative. But if they are due to thermal processes wich are dependent on a plasma temperaature which can vary, then they cannot form the basis for a quantitative technique. In this respect, the CO_2 system tested is not such a suitable analytical source as the ruby and NdYAG systems.

In order to assess the analytical capabilities of the technique we have analyzed several well known standard materials. Table III shows the results obtained by visual photoplate analysis of NBS standard 467 using the NdYAG laser. The series of spectra were recorded over the range 0.01–3 nC charge as measured at the monitor of the mass spectrometer. This gives a measure of the ions passing through the instrument and is the conventional method of recording spectra with the spark source.

The concentrations were calculated using an estimated photoplate sensitivity obtained from the matrix isotope ^{58}Fe. No element correction factors were used. Despite the fact that the analysis was made visually, which gives an accuracy of the order of ±50% with the line extinction method, it can be seen that the elemental sensitivities vary over at most a factor 3.

Table V. Visual Analysis of NBS Glass Standard 611 with the MS7/NdYAG Laser (ppm atomic)

Element	Concentration	
	Given	Calculated
U	117	80
Th	119	60
Pb	124	120
Ag	142	200
Sr	354	200
Rb	298	300
Zn	407	400
Cu	418	600
Ni	468	1000
Co	398	400
Fe	492	600
Mn	531	600
Ti	548	1000
K	712	1000
B	1920	600

Table VI. Visual Analysis of Steel Standard NBS 464 with the MS7/CO_2 Laser (ppm atomic)

Element	Concentration	
	Given	Calculated
Pb	54	<4
W	67	<6
Ta	213	<2
Sn	204	180
Ag	16	<4
Nb	223	12
Mo	166	<20
Zr	62	<4
As	134	200
Ge	12	25
Cu	823	500
Co	266	300
Ni	1280	1200
Mn	13200	3000
Cr	840	600
V	3240	400
Ti	47	15
S	350	400
P	307	300
B	255	200

By using element correction factors and microdensitometry of the lines, this accuracy should be improved.

Table IV gives the analysis figures obtained from a Johnson-Matthey copper standard CAO using the NdYAG laser and recorded in the same way as with the steel analysis. The photoplate sensitivity taken was that estimated from the steel analysis and no element correction factors were made.

Table V shows the visual analysis of a nonconducting material, NBS glass standard 611 with the NdYAG laser. The specimen was in the form of a solid disc and the laser fired directly onto the surface. The series of spectra were again recorded over the range 0.01–3 nC charge and plate sensitivity taken from the steel analysis. No element correction factors were used and it can be seen that the accuracy of the results is similar to those of the metallic samples.

Analysis figures obtained with the ruby laser for the same materials have been reported in a previous paper (2), and are very similar in accuracy to those with the NdYAG laser. Table VI gives the analysis results for NBS steel standard 464 using

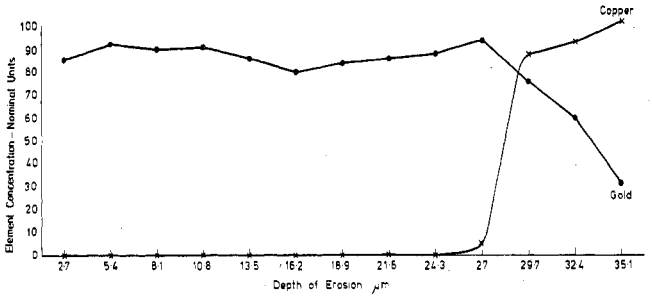

Figure 6. Layer analysis of gold plated brass

the CO_2 laser and shows again the poor comparison and lack of sensitivity for many of the elements.

The results of these and other standard samples examined show that the laser is capable of semiquantitative analysis of many types of materials without a similar type of standard as a comparison.

The reproducibility of element analysis for single laser shot spectra has been measured to be ±20% with the ruby laser which compares favorably with a variation of ±15% in the peak power energy. For the NdYAG laser, reproducibility of analysis was <10% for single shots compared with the manufacturers quoted peak power reproducibility of ±5%. It would be expected that the reproducibility of multiple shot spectra would limit at that of the photoplate emulsion (about ±4%).

In the results we have presented, we have not attempted to demonstrate that the laser source is or can be superior in accuracy to the spark source. This would involve considerably more work to be carried out than has so far been undertaken in these preliminary experiments. First, longer exposures of spectra would be required to be able to densitometer the lines (the human eye is far more sensitive in the detection of a weak line than a photometer) and many more standards would need to be run to determine accurate relative sensitivity factors. Using these methods, there is no reason to doubt that the laser could analyze to an accuracy at present attained by the spark source of about ±10% using photoplates. Electrical detection could improve this further due to its higher sensitivity and more precise measuring capability.

We have so far discussed the use of laser probes mainly from their semiquantitative analysis capability but it must be remembered that the amount of material removed to achieve this accuracy is small. By defocusing the beam, thinner layers can be removed down to approximately 0.2 μm per shot, [Eloy et al. (*5, 6*)]. To demonstrate this, we have examined a specimen of brass sheet, which has a gold layer on the surface, with the ruby laser. The beam diameter was adjusted to 200 μm and the erosion rate of the gold surface was measured to be 0.9 μm per shot. A series of spectra were recorded each spectrum being composed of three laser shots.

Figure 6 shows densitometer measurements of the gold and copper as the laser eroded into the material. It can be seen from the curves that the interface is about 27 μm deep and, by examination of the specimen cross section by microscope, the mean gold depth was measured to be 29 μm.

Each recorded spectrum of three shots gave an element sensitivity of 300 ppm and so all elements present in the layer removed for each spectrum could be detected down to this level. The distribution of elements through surface layers could be measured using this method.

Conversely by focusing the laser to a fine focus, spatial analysis can be obtained across the specimen surface. Line scans or area mapping can be obtained by recording a series of spectra across the area of interest and the photoplate will record all elements above 1000 ppm simultaneously for a single shot. More than one shot in each position will increase the sensitivity according to the number of shots. By using electrical detection, individual elements could be monitored to much lower detection levels and the surface analysis method would be analogous to that undertaken at present by the ion probe.

Solution analysis could be carried out by evaporating the liquid on a flat surface of polythene. With a defocused laser beam, the surface deposit would be analyzed along with some of the polythene but this would only contribute carbon and oxygen lines (assuming high purity material) because of the low molecular formations of the laser source. Higher element sensitivity would be obtained than with the spark source because the liquid deposit would not require mixing with graphite as previously discussed. A moving tape with one or several deposits on the surface could be run through the ion source providing on-line analysis. The laser also offers the possibility of multiple sample loading in the source chamber. This is difficult with the spark source as two small electrodes have to be carefully aligned with each other and the optical axis of the mass spectrometer, and there is thus a danger of contamination from sputtered material. However, with a single specimen which only requires moving into a fixed position for analysis it should be possible to design a source chamber capable of holding several specimens at one loading and to move each one into the analysis position in turn. This would speed up the analysis cycle by saving on the pumping time normally necessary between each sample.

CONCLUSIONS

The laser can now take its place as an analytical source in mass spectrometry for the examination of solid materials. It has been shown to be capable of providing semiquantitative analysis on different types of materials and can produce spectra from unusual specimens such as organic substances. It is yet to be seen if the latter can provide meaningful analytical results.

The laser source competes directly with the conventional spark source in all respects and offers the further advantages of surface analysis, analysis of nonconducting materials, minimal sample preparation, negligible molecular contributions, and simple spectra.

ACKNOWLEDGMENT

The authors wish to note their appreciation to those who loaned laser equipment for these experiments. The CO_2 laser was supplied by GEC-Elliott Automation, Borehamwood, London, England; the ruby laser was supplied by the University of Hull, Hull, England; and the NdYAG laser was supplied by J. K. Lasers, Rugby, England. The authors also acknowledge the keen interest in the work shown by S. A. Ramsden and G. J. Pert of the Department of Applied Physics, The University of Hull.

LITERATURE CITED

(1) A. J. Ahearn, "Mass Spectrometric Analysis of Solids", Elsevier, Amsterdam, 1966, p 5.
(2) R. A. Bingham and P. L. Salter, *Int. J. Mass Spectrom. Ion Phys.*, to be published.
(3) J. F. Ready, "Effects of High Power Laser Radiation", Academic Press, New York; Library of Congress Catalog Card No. 77-137597.
(4) P. R. Pearson and H. M. Lamberton, IEEE/USA, Conference on Laser Engineering and Applications, Washington, D.C. June 2–4, 1971, *IEEE J. Quantum Mechanics*, Special Conference Issue.
(5) J. F. Eloy and J. L. Dumas, *Methods Phys. Anal.*, **2**, 251, (1966).
(6) J. F. Eloy, *Methods Phys. Anal.*, **5**, 157 (1969).

RECEIVED for review February 26, 1975. Accepted April 19, 1976. One of the authors (PLS) acknowledges the receipt of a Science Research Council C.A.S.E. studentship during the period in which this work was carried out and is based on work supported in part by A.W.R.E., Procurement Executive, Ministry of Defence.